ORIGINAL PAPER

K. Gurunathan · P. Maruthamuthu

$Bi_5Nb_3O_{15}$ as a photocatalyst: photocatalytic and photoelectrochemical studies

Abstract $Bi_5Nb_3O_{15}$ was prepared from a stoichiometric mixture of Bi_2O_3 and Nb_2O_5 at 300–500 °C. The prepared photocatalyst was characterized by diffuse reflection spectrum (DRS), X-ray diffraction (XRD), scanning electron microscopy (SEM) and particle size analysis. The band gap, crystal structure and average grain size were determined from the above methods to be 3.25 eV, distorted pyrochlore and 4–5 μm respectively. The photoelectrochemical behavior of hydrogen-reduced $Bi_5Nb_3O_{15}$ was investigated in 0.1 M Na_2SO_4 and using the $Fe(CN)_6^{3-/4-}$ redox couple for measuring the current-voltage characteristics. The cyclic voltammetric studies revealed that the onset potential for photocurrent generation existed at −0.45 V, which is more negative to water reduction level at pH 7.0, and that of the photocurrent at 1.0 V was observed as 0.58 mA/cm^2. Photocatalytic hydrogen production has been achieved by using $Bi_5Nb_3O_{15}$ as a photocatalyst in presence of methyl viologen. The quantum yield for hydrogen production for this system was found to be 0.83. All the studies clearly indicated that $Bi_5Nb_3O_{15}$ has potential in solar energy conversion.

Key words Bismuth-based ternary oxides · Semiconductors · Photocatalysis · Photoelectrochemistry · Solar energy conversion

Introduction

The past two decades have witnessed great efforts worldwide to develop new and efficient photocatalytic

K. Gurunathan (✉)[1] · P. Maruthamuthu
Department of Energy, Madras University,
Guindy Campus, Madras-600 025, India

[1]*Present address*:
Centre for Materials for Electronics Technology,
Panchawati, off Pashan Road, Pune 411 008, India
Electrochemical Materials Science Division,
Central Electrochemical Research Institute,
Karaikudi-630 006, India

and photoelectrochemical systems involving semiconductors for generating fuels and electricity with utilization of the inexhaustible energy source, solar radiation [1–3]. In our laboratory, we have achieved photocatalytic hydrogen production using undoped/doped WO_3, γ-Bi_2O_3, α-Fe_2O_3 and SnO_2 in presence of methyl viologen (MV^{+2}) [4–7]. Of the various semiconductors, the oxide semiconductors show promising results owing to their inherent stability in both acidic and alkaline media. Many binary oxides such as Bi_2O_3, WO_3, TiO_2, ZnO, Fe_2O_3 etc. and ternary oxides such as $SrTiO_3$, $NiTiO_3$ etc. were utilized in devising photoelectrodes for photoelectrochemical solar energy conversion [3]. Of the mixed oxides, sodium hexatitanate, $Na_2Ti_6O_{13}$, with a tunnel structure, when loaded with oxidized Ru, has been found to be an efficient photocatalyst for water decomposition [8].

$BaTi_4O_9$ synthesized by the sol-gel process exhibits photocatalytic activity for water decomposition [9]. Niobium-containing mixed metal oxides are of wide interest and have found a prominent place in this field. The photocatalytic decomposition of H_2O_2 to produce H_2 and O_2 over NiO-$K_4Nb_6O_{17}$ powder, which behaves as an ion-exchanging layered compound, is reported to proceed steadily for a duration of more than 50 h under band gap irradiation [10]. CdS-loaded $K_4Nb_6O_{17}$ shows photocatalytic activities for hydrogen evolution from aqueous K_2SO_3 solution under visible light irradiation [11]. Some layered niobates and titanoniobates such as KNb_3O_8 and $CsTi_2NbO_7$ and $K_4Nb_6O_{17}$ show high photocatalytic activities for hydrogen evolution from aqueous methanol solution [12, 13]. Photoluminescence and photocatalytic hydrogen evolution reactions of layered caesium titanates, $Cs_2Ti_nO_{2n+1}$ (n = 2, 5, 6) have been studied to evaluate the photoactivity of these materials [14]. The photoelectrochemical behaviour of reduced $Ni_2Nb_2O_6$ single-crystal electrodes and its sintered pellets has been studied in 1 M sodium acetate by measuring their *I–V* characteristics and spectral response [15]. Domen et al. have reported complete water splitting with $K_4Nb_6O_{17}$ [16]. Photoelectrochemical studies of $\gamma - Bi_2O_3$ doped with transition metal ions in

$Fe(CN)_6^{3-/4-}$ and $MV^{2+}/MV^{\cdot+}$ and in presence of Na_2SO_4 as a supporting electrolyte were carried out in our laboratory [17, 18].

Ramakrishnan et al. [19] have investigated the photo-electrochemical properties of oxide bronze Ba_3Nb_4-Ti_4O_{21} in NaOH electrolyte. In accord with the above results, $Bi_5Nb_3O_{15}$ prepared and studied in our laboratory exhibited a good photoresponse. In fact, photocatalytic and photoelectrochemical studies on $Bi_5Nb_3O_{15}$ used as a photoanode are reported for the first time in this article.

Experimental

Bi_2O_3 and Nb_2O_5 of purity $> 99.5\%$ were procured from Fluka Switzerland and methyl viologen dichloride hydrate (MV^{2+}: 1,1′-dimethyl-4,4′-bipyridinium dichloride) was purchased from Aldrich, USA. All other chemicals used were of research grade.

Preparation and characterization of $Bi_5Nb_3O_{15}$

The ternary oxide photocatalyst, $Bi_5Nb_3O_{15}$ was prepared from a stoichiometric mixture of Bi_2O_3 and Nb_2O_5. The mixture was sintered at 300–500 °C in air for 12 h and then cooled to room temperature slowly. The catalyst was ground to a fine powder and stored in an air-tight bottle with protection from light.

Characterization

The prepared photocatalyst was characterized by spectral, optical and other physical methods. The diffuse reflection spectrum was recorded with a Varian spectrophotometer (Model Cary 2300) equipped with an integrating sphere and $BaSO_4$ as a white standard. XRD measurements of the oxide crystal were made with computer-controlled Philips equipment (X-Ray generator PW 1130; Vertical diffractometer PW 1710) using CuK_α radiation of $\lambda = 1.5405$ Å. To examine the surface morphology and the particle size of the catalyst powder, SEM photographs were taken with a JEOL instrument, model JSM 35 CF. Surface area, as measured with a Quantasorb surface area analyzer, was 5 m²/g. The particle size distribution was determined by laser diffraction particle size analysis (Malvern Instruments, model 3600 Ec) using He-Ne laser radiation (632.8 nm) in sodium pyrophosphate-water (1.35 g/l).

Photocatalytic experimental set-up

The photocatalytic experimental set-up is reported by us in our earlier studies [5]. The photocatalyst powders (100 mg) were dispersed in 100 ml of MV^{2+} ($[MV^{2+}] = 4.0 \times 10^{-5}$ mol dm^{-3}) in a double-walled photo-reactor with water inlet and outlet to maintain the temperature at 25 °C by circulation of water, deaerated with argon for 1 h and illuminated by a 450-W tungsten-halogen lamp. UV and IR radiations were cut off by using a 380-nm filter and water jacket, respectively, prior to irradiation of the sample. The evolved gas was passed through alkaline pyrogallol solution at 0–5 °C to remove oxygen (if formed due to water oxidation by valence band holes, h_{vb}^+), and the rest of the gas was collected in a water manometer. The collected gas was detected as hydrogen by GC (Chromatography and Instruments Company, CIC, India) using a Porabak Q column and argon as the carrier gas.

Quantum yield estimation

Quantum yields for photocatalytic hydrogen production have been reported by us earlier [6] and, adopting the same procedure for the present system using $Bi_5Nb_3O_{15}$ as a photocatalyst, were calculated by using the following formula:

$$\text{Quantum yield } (\phi_{H_2}) = \frac{2 \times H_2 \text{ rate (M s}^{-1})}{\text{Photon rate (Einsteins/cm/s)}} \quad (1)$$

The denominator in Eq. 1 is derived as follows. The basic equation for ϕ is

$$\phi = \frac{\text{Number of } H_2 \text{ atoms formed per second}}{\text{Number of photons absorbed per second}} \quad (2)$$

From the diffuse absorption spectrum, the absorption of $Bi_5Nb_3O_{15}$ at 380 nm is found for the quantum yield calculation. The actual number of photons coming into the slurry was calculated as

Number of Einsteins absorbed per sec

$$= \frac{I_0 \times \% \text{ of absorption at 380 nm}}{100} \quad (3)$$

where $I_0 =$ intensity of incident light.

Electrode preparation

Pellets of size 10 mm diameter by 1.5 mm thickness were made from the catalyst powder and were sintered, first in air at 500 °C for 18 h to improve their hardness and then in a hydrogen atmosphere at 300 °C for 30 min to enhance their conductivity. After polishing, they were etched with 5% HNO_3 and rinsed in distilled water. Ohmic contact was made on one face of the pellet with In-Ga eutectic alloy, and a Cu wire was connected to this side with Ag paint. After drying in a vacuum oven at 110 °C, they were mounted on a glass tube using epoxy resin and were used as photoanodes. The cylindrical vessel was made up of Pyrex glass with an optical window in the front and inert gas inlet and outlet.

Electrochemical experimental set-up

A three-electrode system involving the photoanode (working electrode, WE), 1 cm² Pt foil counter electrode and Ag/AgCl reference electrode was employed. Experiments were conducted with an "Electrochemical Analyzer" (BAS 100-A model, USA). The recording device consists of a Houston instrument (Austin, USA) Model DMP-40 plotter and a Panasonic Impact dot-matrix printer (Model kX-P 1180). The source of excitation was a 450-W xenon arc lamp (Photon Technology International, Princeton, USA). The lamp housing was water-cooled (by ice water circulation at 500 ml/min) and sealed so that a venting system was not required. Heat from the lamp was dispersed by filtering the radiation through the circulating water. The light was chopped by an optical chopper (Model OC-4000, PTi, Princeton, USA). Photocurrent and photovoltage were measured with a Keithley 614 Electrometer. The radiation from the 450-W xenon arc lamp was passed through a monochromator (Applied Photophysics, London) and a 380-nm cut-off was introduced into the path of the excitation beam for selecting the excitation wavelengths. The light intensity from the xenon lamp at 380 nm was determined by the ferrioxalate actinometry [20] method and was found to be 1.70×10^{-8} Einsteins $\cdot$ cm$^{-2} \cdot$ s^{-1}. I–V measurements were made under dark and chopped light-irradiated conditions. All photoelectrochemical measurements were carried out under a nitrogen atmosphere at 25 °C.

Results and discussion

Characterization

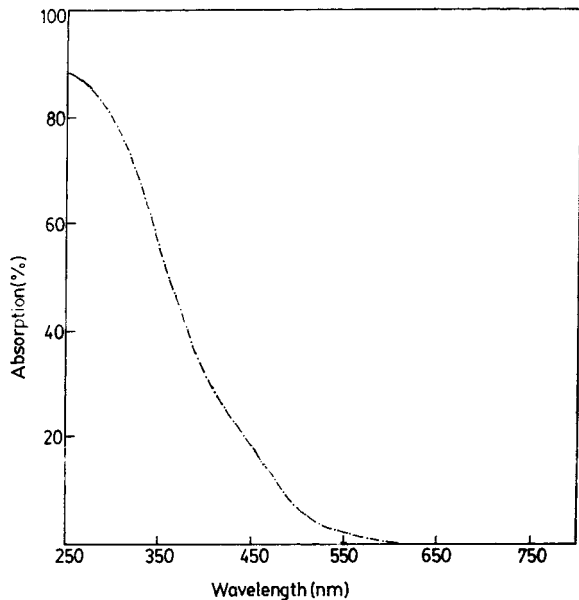Figure 1 shows the diffuse absorption spectrum of $Bi_5Nb_3O_{15}$ derived from the corresponding diffuse re-

Fig. 1 Diffuse absorption spectrum of $Bi_5Nb_3O_{15}$

Table 1 XRD data of $Bi_5Nb_3O_{15}$

Theoretical value		Observed value	
'd' spacing (Å)	I/I_0	'd' spacing (Å)	I/I_0
3.11	100	3.11	100
2.73	35	2.73	51
2.62	20	2.62	10
1.93	20	1.93	16
1.89	25	1.89	29
1.64	20	1.64	31
1.59	12	1.59	7
1.56	8	1.54	11
1.36	4	1.36	8

O_{15}. From this table, it can be seen that the particle size (percentages are in parentheses) of $Bi_5Nb_3O_{15}$ at 4.1 μm (25.8%) 4.7 μm (40.4%) and 5.4 μm (30.6%) are distributed in various bands. From the above data, it can be seen that the major particle size distribution is around 4–5 μm.

flectance spectrum. As seen in Fig. 1, the band edge occurs at 380 nm, which closely matches the band gap energy of 3.25 eV. There are no other states in the band gap. The individual oxides, Bi_2O_3 and Nb_2O_5, however, do not exhibit any characteristic spectra. The X-ray diffractogram of the catalyst displayed in Fig. 2 shows that it has a distorted pyrochlore structure, and, further, the observed 'd' spacing values are in close agreement with the theoretical values [21]. The XRD data of $Bi_5Nb_3O_{15}$, both theoretical and observed values, are presented in Table 1. $Bi_5Nb_3O_{15}$ is the homologous series formed by intergrowth of n = 1 and n = 2 like units of the Aurivillus family [22]. Figure 3 illustrates the scanning electron micrograph which explicitly indicates that the crystallites are smooth and homogeneous at their surface and their grain boundaries are reduced. Also the, grains appear to have a cauliflower structure, and the average grain size is in the range 4–5 μm. Table 2 presents the particle size distribution of Bi_5Nb_3

Photocatalytic hydrogen production using $Bi_5Nb_3O_{15}$

Photocatalytic decomposition of water into its components (H_2 and O_2) is an important method for solar energy conversion and to characterize the photocatalysts. We have attempted photocatalytic hydrogen production using $Bi_5Nb_3O_{15}$ in the presence of methyl viologen. Table 3 presents the amount of photocatalytic hydrogen produced with time using $Bi_5Nb_3O_{15}$ as a photocatalyst and aqueous methyl viologen as an electron relay. From Table 3, we see that hydrogen production increases with increase in time and reaches the saturation level. There is no hydrogen evolution without $Bi_5Nb_3O_{15}$ and methyl viologen. The reaction mechanism for photocatalytic hydrogen production using a semiconductor and aqueous methyl viologen was reported by us earlier [5–7]. The quantum yield for photocatalytic hydrogen production using $Bi_5Nb_3O_{15}$ at 380 nm is 0.83.

Fig. 2 XRD of $Bi_5Nb_3O_{15}$
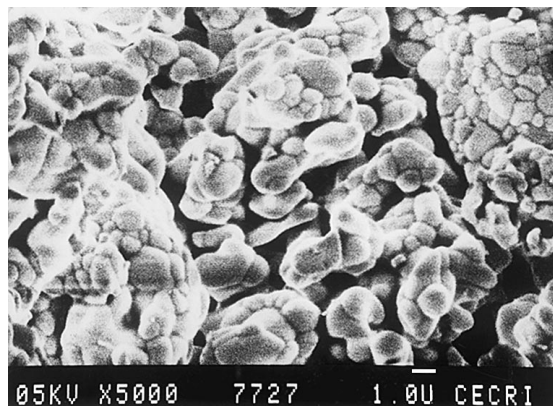
Fig. 3 Scanning electron micrograph of $Bi_5Nb_3O_{15}$

Photoelectrochemical study

Photoelectrochemical (PEC) studies are another tool to characterize the prepared semiconductor photocatalyst. As the catalyst had a high resistivity (1.1×10^4 Ω cm), it is necessary to enhance its conductivity prior to photoelectrode preparation. The as-sintered pellets of $Bi_5Nb_3O_{15}$ are white in color. Electronic conductivity could be induced in $Bi_5Nb_3O_{15}$ only by hydrogen, and hence photoelectrochemical studies could be carried out on hydrogen-reduced $Bi_5Nb_3O_{15}$. The phase of $Bi_5Nb_3O_{15}$ is stable after hydrogen reduction; this was confirmed by XRD. The reduced pellets of $Bi_5Nb_3O_{15}$ are slightly black in color, indicating the creation of donor levels of Bi^{2+}/Nb^{4+}. The room temperature resistivity of the hydrogen-reduced pellets of $Bi_5Nb_3O_{15}$, measured using a two-probe apparatus, were in the range 800–900 Ω cm. The hydrogen-treated pellets were employed in the photoelectrode construction as detailed in the experimental part.

A maximum value of the open-circuit photovoltage of 614 mV vs Ag/AgCl was observed. By the hot-probe method, $Bi_5Nb_3O_{15}$ is confirmed as an n-type semiconductor. Figure 4 exhibits the photocurrent behavior of $Bi_5Nb_3O_{15}$ as a function of applied voltage in 0.1 M Na_2SO_4 solution. The anodic dark current is less, but a significant photocurrent is generated on illumination of the photoanode (at 380 nm) at -0.35 V vs Ag/AgCl. The

Table 2 Particle size distribution of $Bi_5Nb_3O_{15}$

Particle size (μm)	Distribution band (%)
2.6	0.0
3.0	0.2
3.5	1.1
4.1	25.8
4.7	40.4
5.4	30.6
6.3	1.1
7.3	0.0
8.5	0.0
9.8	0.0

Table 3 Photocatalytic hydrogen production using $Bi_5Nb_3O_{15}$ in presence of methyl viologen; $[MV^{2+}] = 4.0 \times 10^{-5}$ mol dm^{-3}; temperature = 25 °C

Time (min)	Amount of H_2 evolved (μM)
0	0.00
10	2.68
20	5.35
30	8.47
40	8.92
50	11.60
60	13.38
70	13.38

shift towards more negative potential for photocurrent generation also proved that $Bi_5Nb_3O_{15}$ is an n-type semiconductor.

The photocurrent onset potential of -0.35 V vs Ag/AgCl gives a rough estimate of the flat-band potential, V_{fb}. The flat-band potential is the electrode potential at which there is no band bending in the semiconductor electrode and is a property of the specific electrode/electrolyte interface. This is an important parameter, and, since it is measured at zero current, the value is numerically equal to the minimum applied voltage required to decompose water using the semiconductor.

The photoelectrochemical behaviour of $Bi_5Nb_3O_{15}$ with a $Fe(CN)_6^{3-/4-}$ redox couple and Na_2SO_4 electrolyte is illustrated in Fig. 5. The onset potential (V_{fb}) lies at -0.35 V, which is obvious in the figure. Here, the anodic dark current is less and a maximum photocurrent of 0.75 mA is reached at 1.0 V. In Figs. 5 and 6, we show manual chopping of light to get a distinct photocurrent. There is no photocorrosion in this system, which is evident in Figs. 4 and 5. The quantum efficiency for the conversion of light to electrical energy was found to be 2.6 for the above system.

The cyclic voltammetric studies of $Bi_5Nb_3O_{15}$ in the presence of the $Fe(CN)_6^{3-/4-}$ couple and 0.1 M Na_2SO_4 under dark and manually chopped light illumination conditions are represented in Fig. 6. The onset potential is at -0.45 V vs Ag/AgCl, which is more negative than
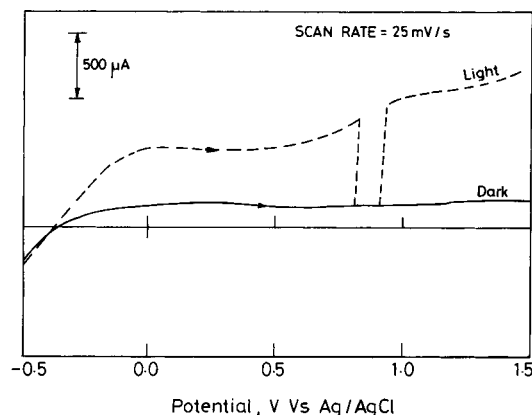

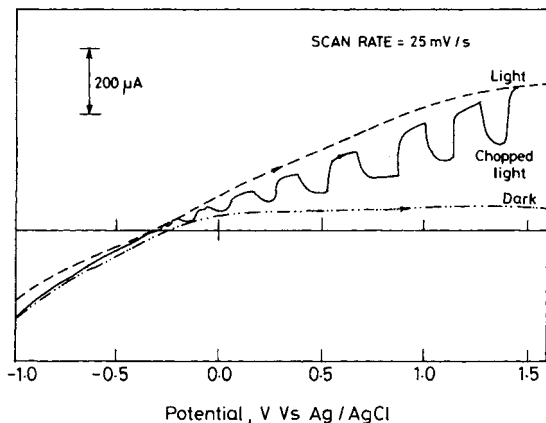**Fig. 4** I–V characteristics of $Bi_5Nb_3O_{15}$ in 0.1 M Na_2SO_4

Fig. 5 Photoelectrochemical behavior of $Bi_5Nb_3O_{15}$ in $Fe(CN)_6^{3-/4-}$ and 0.1 M Na_2SO_4 solution. $[Fe(CN)_6^{3-}] = 5 \times 10^{-3}$ mol dm^{-3}; $[Fe(CN)_6^{4-}] = 1 \times 10^{-2}$ mol dm^{-3}
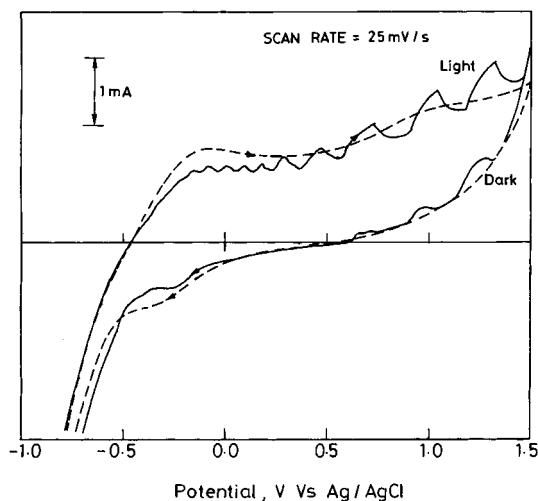

Fig. 6 Cyclic voltammetric studies of $Bi_5Nb_3O_{15}$ under chopped illumination in 0.1 M Na_2SO_4 solution

the water reduction value (i.e. −0.41 V) at pH 7.0. The maximum photocurrent of 0.58 mA/cm^2 observed at 1.0 V vs Ag/AgCl.

Conclusions

The prepared $Bi_5Nb_3O_{15}$ photocatalyst has a band gap of 3.25 eV, and its structure is distorted pyrochlore with a particle size of 4–5 µm. From the cyclic voltammetric studies, it was observed that the onset potential (flat-band potential) was at about −0.45 V vs Ag/AgCl, which is more negative than the water reduction value. The quantum yield for photocatalytic hydrogen production using $Bi_5Nb_3O_{15}$ is 0.83. In conclusion, $Bi_5Nb_3O_{15}$ is one of the photocatalysts for the water splitting reaction in the near-visible region of solar light.

References

1. Gratzel M (ed) (1983) Energy resources through photochemistry and catalysis. Academic Press, New York
2. Pleskov Yuri V (ed) (1990) Solar energy conversion, a photoelectrochemical approach. Springer, Berlin Heidelberg New York
3. Rajeswar K (1985) J Appl Electrochem 15: 1
4. Maruthamuthu P, Gurunathan K, Subramanian E (1990) Bull Electrochem 6: 128
5. Maruthamuthu P, Gurunathan K, Subramanian E, Sastri MVC (1993) Int J Hydrogen Energy 18: 9
6. Gurunathan K, Maruthamuthu P (1995) Int J Hydrogen Energy 20: 287
7. Gurunathan K, Maruthamthu P, Sastri MVC (1997) Int J Hydrogen Energy 22: 57
8. Inoue Y, Kubokawa T, Sato K (1990) J Chem Soc Chem Commun: 1298
9. Kohno M, Ogura S, Inoue Y (1996) J Mater Chem 6: 1921
10. Kudo A, Tanaka A, Domen K, Maruya K, Aika K, Onishi T (1988) J Catalysis 111: 67
11. Yoshimura J, Tanaka A, Konda J, Domen K (1995) Bull Chem Soc 68: 2439
12. Domen K, Kudo A, Shinozaki A, Tanaka A, Maruya K, Onishi T (1986) J Chem Soc Chem Commun: 356
13. Sekine T, Yoshimura J, Tanaka A, Domen K, Maruya K, Onishi T (1990) Bull Chem Soc 63: 2107
14. Kudo A, Konda T (1997) J Mater Chem 7: 777
15. Guochang L, Bicelli LP, Razzini (1991) Sol Energy Mater 21: 335
16. Domen K, Kudo A, Shinozaki A, Tanaka A, Maruya K, Onishi T (1986) J Chem Soc Chem Commun: 1706
17. Ramakrishnan PA, Sampath S, Subba Rao GV (1993) Mater Chem Phys 34: 295
18. Gurunathan K (1993) PhD thesis, University of Madras
19. Gurunathan K, Maruthamuthu P (1994) Electrochem Soc Inc 186th Meeting. Extended Abstr 2: 791
20. Hatchard CG, Parker CA (1956) Proc Roy Soc A235: 518
21. ASTM card No. 16–0293
22. Gopalakrishnan J, Ramanan A, Rao CNR, Jefferson DA, Smith DJ (1984) J Solid State Chem 55: 101